Published by IOP Publishing for Sissa Medialab
Received: *January 23, 2020*
Accepted: *March 4, 2020*
Published: *April 14, 2020*

International Workshop on Fast Cherenkov Detectors
Photon detection, DIRC design and DAQ
September 11–13, 2019, Giessen, Germany

# Overview of PID options for experiments at the Super Charm-Tau Factory

**A.Yu. Barnyakov,**[a,b,c,1] **M.Yu. Barnyakov,**[a,c] **M.S. Belozyorova,**[a,b] **V.S. Boborovnikov,**[a,b] **A.R. Buzykaev,**[a,b] **A.F. Danilyuk,**[b,d] **A.A. Katcin,**[a,b] **S.A. Kononov,**[a,b] **E.A. Kravchenko,**[a,b] **I.A. Kuyanov,**[a,b] **A.P. Onuchin,**[a,b] **I.V. Ovtin,**[a,b] **I.M. Plekhov,**[a,b] **N.A. Podgornov,**[a,b] **G.P. Razuvaev,**[a,b] **K.Yu. Todyshev**[a,b] **and V.S. Vorobyev**[a,b,e]

[a]*Budker Institute of Nuclear Physics,*
*pr. Lavrentieva 11, Novosibirsk, Russia*
[b]*Novosibirsk State University,*
*st. Pirogova 2, Novosibirsk, Russia*
[c]*Novosibirsk State Technical University,*
*pr. Karla Marksa 21, Novosibirsk, Russia*
[d]*Boreskov Institute of Catalysis,*
*pr. Lavrentieva 5, Novosibirsk, Russia*
[e]*Lebedev Physical Institute,*
*pr. Leninskii 53, Moscow, Russia*

*E-mail:* a.yu.barnyakov@inp.nsk.su

Abstract: The Super Charm-Tau Factory is an electron-positron collider project in Novosibirsk with a peak luminosity of $10^{35}\,\mathrm{cm^{-1}s^{-1}}$ operating in the center of mass energy range between 2 and 6 GeV. The physics program of the experiment in general is devoted to the study of charm quark and tau lepton. Conceptual designs of the collider and a universal detector are presented. The dedicated particle identification (PID) system is required to provide the state-of-the-art level of $\mu/\pi$ separation for the particle momenta up to 1.2 GeV/c. The following options for the PID system are considered in this paper: Focusing Aerogel RICH (FARICH) detector composed of 4-layer aerogel tiles, threshold Cherenkov counters based on aerogel and shifter (ASHIPH), Focusing DIRC (FDIRC) counter and time-of-flight (ToF) detector combined with the time-of-propagation (ToP) approach providing a time resolution better than 30 ps. Also the capabilities of particles separation in tracking system are discussed. Comparison of PID approaches with help of parametric simulation is performed.

Keywords: Particle identification methods; Cherenkov detectors; Particle tracking detectors; Timing detectors

[1]Corresponding author.


https://doi.org/10.1088/1748-0221/15/04/C04032

2020 JINST 15 C04032

## Contents


**1 Introduction** **1**

**2 Collider and Detector concept** **2**

**3 Particle identification** **4**
- 3.1 Tracking system 4
- 3.2 FARICH 5
- 3.3 Threshold aerogel Cherenkov counters ASHIPH with SiPM 6
- 3.4 DIRC-like and ToF options 7

**4 Comparison of PID system options** **8**

**5 Summary** **9**


# 1 Introduction

The Super Charm-Tau (SCT) Factory is a project of $e^+e^-$ collider with a peak luminosity of $10^{35}\,\mathrm{cm}^{-1}\mathrm{s}^{-1}$ operating in the center of mass energy range between 2 and 6 GeV [1]. The goal luminosity of the collider will exceed 100 times the luminosity of BEPC-II (Beijing Electron-Positron Collider, China) [2], which is under operation today in the same energy range. The other feature of the project is a high level (80–90%) of longitudinal polarization of the electron beam at the interaction point. The proposed collider machine with high luminosity and beam longitudinal polarization combined with a high performance universal detector will allow us to provide a series of precise experiments and tests of the Standard Model (SM).

In figure 1 the ratio ($R$) of hadron production cross-section to muon production cross-section is shown for the energy range of the Novosibirsk SCT Factory. The operation energy range from 2 GeV to 6 GeV will cover the thresholds of $\tau$-lepton production and almost all charmed states up to the region of $\Omega_c$-baryon. The physics program of the experiment is devoted to the measurements of charm quark and tau lepton. It includes precision tests of the SM in the electro-weak sector (lepton flavor universality tests, measurement of the CKM matrix elements, measurements of the weak charged current structure in tau decays), QCD measurements in the non-perturbative region (hadronic cross sections, spectroscopy, dynamics of the hadronic decays of the charmed hadrons and tau lepton), and searches for the beyond SM phenomena (lepton flavour violating decays and other forbidden or highly suppressed processes in the SM).

During 10 years of operation of the SCT factory the integrated luminosity will be about $10\,\mathrm{ab}^{-1}$, therefore $N_{\tau^+\tau^-}$ could reach $2 \times 10^{10}$. This number of $\tau$-leptons will not exceed the number expected in the Belle-II experiment. But some feasibility studies demonstrate that the sensitivity of the SCT factory project to $\tau$-lepton physics will be better than at the Super-B factory and at proton colliders. For instance, the sensitivity to search for $\tau \to \mu\gamma$ process (LFV in $\tau$-decay) at the SCT factory will be 10 times better than at the Belle-II due to better kinematics of the $\tau$ near the threshold of production and due to good $\mu/\pi$-separation in a dedicated PID system [3, 4]. The longitudinal polarization of the electron beam to better than 50% will help to perform more accurate measurements of the $\tau$-lepton Michel parameters than expected at the Super-B factory [5] and Weinberg angle measurement at the energy of the J/$\psi$-meson [6]. Other feasibility studies for various physics cases are now under consideration [7].

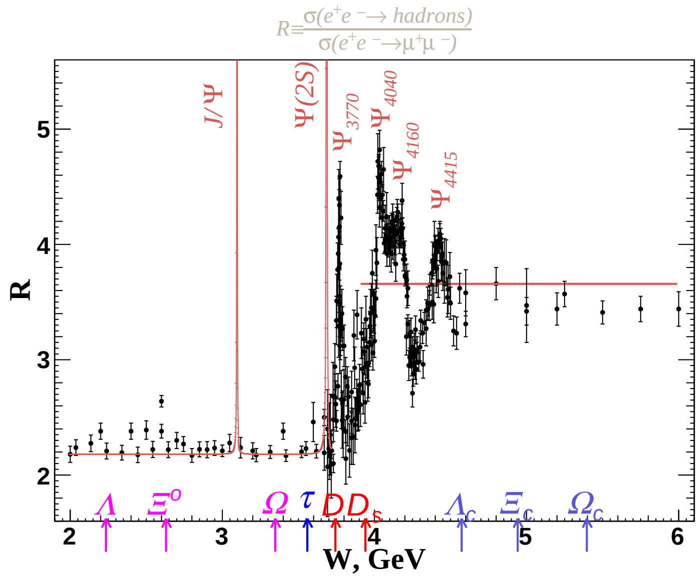


**Figure 1**. *R* ratio for Super Charm-Tau Factory operation energy range. Red line is an approximation of the experimental data from PDG with two Breight-Wigner peaks and constant level [8]. Arrows at x-axis show the energy of double-production of the particles referenced above the axis.

## 2 Collider and Detector concept

The future SCT factory is a symmetric double ring $e^+e^-$ collider. The high single-bunch luminosity is achieved by implementation of a Crab-Waist collision scheme with a large Pivinsky parameter and submillimeter $\beta_y$ (vertical beta-function) in the interaction region. The estimated effect from implementing the new collision scheme for the SCT factory is about a factor of 100 in comparison with the traditional one which is used at the Chinese C-$\tau$ factory BEPC-II (IHEP) [2]. The first collider concept was developed in 2011 and its main parameters are presented in [9]. In 2019 the concept of the accelerating complex was updated. The sketch of the collider rings and major changes are presented in figure 2 (left). Another feature of the SCT factory project in Novosibirsk is a longitudinal electron beam polarization in the interaction region. It is shown in [10] that the level of 80-90% electron beam polarization for beam energy range below 2.2 GeV is achievable with the help of three Sibirian Snake spin rotators, whereas 50% polarization at 3 GeV is expected in this scheme.

The sketch of a universal magnetic detector proposed for the SCT factory project is shown in figure 2 (right). The common requirements for the detector from the physics program and collider parameters are the following:



2020 JINST 15 C04032

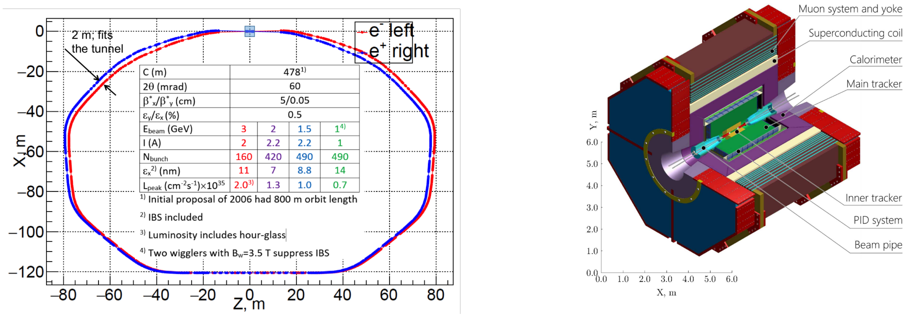


**Figure 2**. Schematic view of collider and its main parameters (left) and detector and its systems (right).

- axial magnetic field of 1–1.5 T;
- for charged particles momentum resolution $\frac{\sigma_P}{P} \leqslant 0.4\%$ at 1 GeV/$c$;
- good symmetry and hermeticity;
- soft track detection (with momenta from 50 MeV/$c$);
- $\mu/\pi$-separation up to 1.2 GeV/c and $\pi/K$-separation up to 2.5 GeV/c at the level of 3 standard deviations ($\sigma$);
- good $\pi^0/\gamma$-separation and $\gamma$ detection with $E_\gamma = 10 \div 3000$ MeV;
- energy measurement resolution $\frac{\sigma_E}{E} \leqslant 1.8\%$ at 1 GeV;
- fast enough readout electronics to work with trigger rate up to 300 kHz.

In the modern concept of the detector the tracking system is divided in two parts: inner tracker to detect soft tracks and main tracker based on Drift Chamber (DC). For the inner tracker several different options are under consideration: Si-strip 4-layer detector, cylindrical GEM (Gas Electron Multiplayer) and TPC (Time-Projection-Chamber) [11]. The main limitation for use of different options close to the interaction region comes from physics background (BhaBha scattering and two gamma production of $e^+e^-$ pairs). First results of the physics background simulation for the SCT factory project are presented in [12]. For DC there are two proposals. One of them is called "traditional" which is based on hexagonal drift cell with size $6 \div 7.5$ mm, 41 layers combined into 10 super-layers with alternating axial and stereo layers [13]. The second proposal is called "ultra low mass DC" with rectangular cell $7.2 \times 9.3$ mm$^2$, 64 stereo layers, total number of very thin wires is about 100 000 [14]. In both cases if the readout electronics will provide the single ionization clusters counting it could help to improve the $\frac{dE}{dx}$-resolution approximately by two times and extend the momentum range for reliable particle identification with help of the trackig system (see section 3.1). A dedicated PID system is needed to provide $\pi/K$- and $\mu/\pi$-separation with more than $3\sigma$ level in momentum ranges 0.6–2.5 GeV/$c$ and 0.2–1.2 GeV/$c$, respectively. Detailed discussion on the PID system is presented in section 3. The main tasks of electromagnetic calorimeter are to provide good $\pi^0/\gamma$-separation and detection of $\gamma$-quanta with $E_\gamma = 10 \div 3000$ MeV. Also the calorimeter should be fast ($\sigma_t \leqslant 1$ ns and small shaping time) to suppress beam background and pileup noise.



2020 JINST 15 C04032

Therefore as a base option the calorimeter based on pure CsI crystals with decay time about 36 ns is considered. The recent R&D at BINP shows that light output from the CsI-crystals could be increased almost by 6 times by using 4 avalanche photodiodes (APD) and wavelength shifter (WLS) with specific shapes [15]. To separate muons from hadrons the muon system placed in the 9 gaps of the yoke iron will be used. The option of the muon system for the SCT factory project based on scintillating plastic and WLS fibre coupled to SiPMs (Silicon Photomultiplayers) is being developed in LPI (Moscow). Some details and R&D progress are presented in [16].

## 3 Particle identification

An excellent particle identification is needed for success of the broad experimental program especially for study of rare processes or the search of phenomena beyond the SM. For low momenta particles it is possible to use measurements of energy deposition for ionizing loss in the tracking system, while to cover the whole operational particle momenta range a special dedicated PID system is required. To study D-meson states the separation of $\pi$- and K-mesons is needed over the whole operational momenta range. For the search of $\tau \to \mu\gamma$ decay a perfect $\mu/\pi$-separation is required in momenta range from 0.5 to 1.2 GeV/c [3, 4], while in semi-leptonic D-meson decays half of muons and pions will have momenta below 0.4 GeV/$c$. It is more complicated to provide good (at the level of more than $3\sigma$) $\mu/\pi$-separation than $\pi/K$- or $K/p$-separation in the operational momenta range of the SCT factory. Therefore the PID approaches are considered in this work mainly from the point of view of excellent $\mu/\pi$-separation.

### 3.1 Tracking system

In [11] it is shown that $\mu/\pi$-separation in momenta range from 55 to 80 MeV/$c$ is available only in the inner tracker ($R \leqslant 20$ cm) with two options: Si-strip detector and TPC. Due to the magnetic field of the detector (1.5 T) the particles with transverse momenta below 180 MeV/$c$ will not traverse the DC ($R \leqslant 80$ cm) in the barrel part of the detector. Therefore the tracking system should be optimized to provide the reliable $\mu/\pi$-separation below 180 MeV/c. Due to recent progress in fast digitizing electronics two operation modes of DC could be considered for modern and future experiments. The traditional mode (commonly used in DCs today and before), when only the first ionization cluster in a drift cell is detected, and the cluster counting mode, when each single ionization cluster is detected. Such approach was implemented in the central drift chamber of the MEG II experiment for the first time [17]. In figure 3 the dependencies of $dE/dx$ on particle momenta is presented. The dependencies were simulated with help of parametric simulation developed for SCT detector software package. The BaBar DC parameters [18] were used in the parametric simulation. In figure 4 the dependencies of number of detected single ionization clusters ($N_{cl}/dx$) on particle momenta is shown. In the parametric simulation the parameters presented in [14] are used: 12.5 single ionization clusters per one cm track from minimal-ionizing particle in gas mixture Helium (He:90%) and isobutane ($iC_4H_{10}$:10%). The evaluated power of separation in terms of $\sigma$ for both approaches are shown in figure 5: $\mu/\pi$-separation with $dE/dx$ approach (•), $\mu/\pi$-separation with $N_{cl}/dx$ approach (•), $\pi/K$-separation with $dE/dx$ approach (□), $\pi/K$-separation with $N_{cl}/dx$ approach (□). It is shown that the cluster counting mode permits to extend the region of reliable $\mu/\pi$-separation ($\geqslant 3\sigma$) up to 220 MeV/$c$.

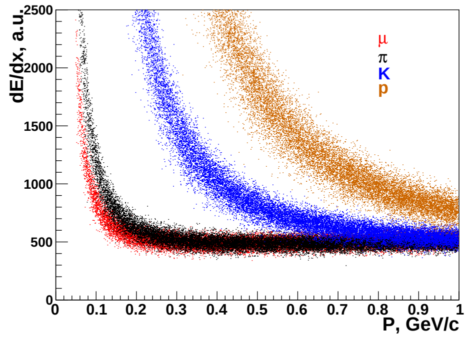


**Figure 3**. Dependencies of ionizing loos energy deposition ($dE/dx$) on particle momenta for muon, pion, kaon and proton from parametric simulation of SCT detector.

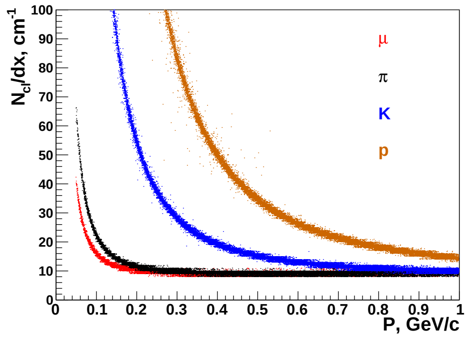


**Figure 4**. Dependencies of single ionization clusters number on particle momenta for muon, pion, kaon and proton from parametric simulation of SCT detector.

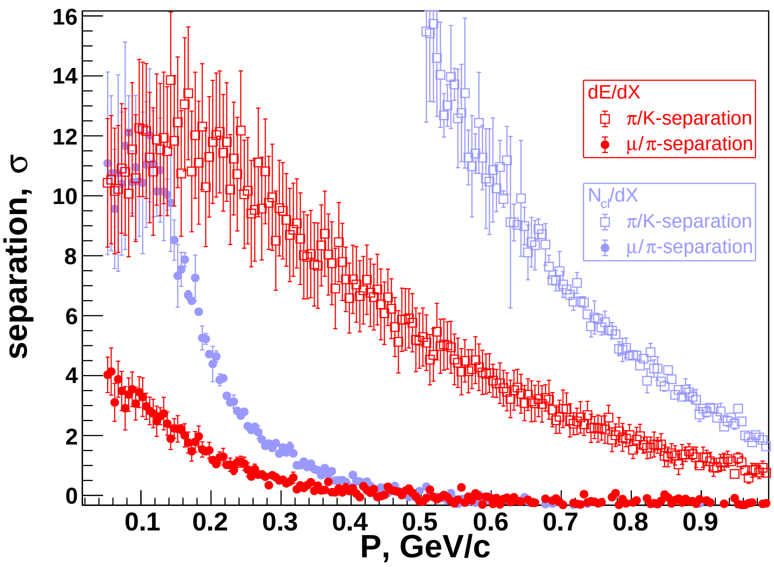


**Figure 5**. Separation power in terms of $\sigma$ on particle momenta: $\mu/\pi$-separation with $dE/dx$ approach (●), $\mu/\pi$-separation with $\mathrm{N_{cl}}/dx$ approach (●), $\pi/K$-separation with $dE/dx$ approach (□), $\pi/K$-separation with $\mathrm{N_{cl}}/dx$ approach (□).

### 3.2 FARICH

The general idea of Focusing Aerogel RICH (FARICH) is to arrange several aerogel layers with different refractive indices ($n$) so that Cherenkov rings from different layers overlap at the photon detector plane. Monolithic 4-layer blocks are more preferable than a stack because there are no additional light losses in the gaps between aerogel blocks due to fresnel reflection and light scattering on the entrance surface of each aerogel block. The first 4-layer aerogel monolithic block was produced in Novosibirsk in 2004 [19]. A similar approach is exploited today in the system ARICH of the Belle-II experiment (Super KEKb, Japan) [20]. The FARICH technique based on

4-layer focusing aerogel with maximal refractive index $n_{\max} = 1.05$ and total thickness 35 mm is able to provide good $\pi/K$-separation in the whole operation momenta region and $\mu/\pi$-separation in momenta range from 0.4 up to 1.5 GeV/$c$ at the level of $3\sigma$. This was demonstrated with simulation and the prototype beam test at CERN in 2012 [21, 22]. Recent results on FARICH R&D are presented in [23]. The use of aerogel with $n_{\max} = 1.07$ could help to extend $\mu/\pi$-separation capability in low momenta region (from 275 MeV/$c$).

The conceptual design of the FARICH system for SCT factory project is based on the following:

- the system cover 98% of the full solid angle (two endcaps and one barrel part);
- 4-layer focusing aerogel radiator with $n_{\max} = 1.07$ and thickness of 35 mm, area of 17 m$^2$;
- distance between input face of the radiator and that of photon detector is 20 cm;
- position sensitive photon detector with $3 \times 3$ mm$^2$ pixel size, area of 21 m$^2$;
- about 1.8 million electronics channels;
- material budget for normal incidence is 15–30% $X_0$ depending on the type of photon detectors.

### 3.3 Threshold aerogel Cherenkov counters ASHIPH with SiPM

The mass-production of the multi-layer focusing aerogel is still a very challenge issue. Due to this circumstance the other PID option based on threshold aerogel Cherenkov counters is considered too. The main idea is to exploit the experience obtained in BINP with operation of two aerogel threshold Cherenkov counter systems based on ASHIPH (Aerogel SHIfter PHotomultiplier) technique [24]: the ASHIPH system for the KEDR detector [25] at the e$^+$e$^-$ collider VEPP-4M and the system for the SND detector [26, 27] at the e$^+$e$^-$ collider VEPP-2000. For the SCT detector project the aerogels with two refractive indexes are considered: n=1.03 ($\mu/\pi$-separation from 0.43 to 0.57 GeV/$c$ and $\pi/K$-separation from 0.57 to 2 GeV/$c$) and n=1.015 ($\mu/\pi$-separation from 0.6 to 0.8 GeV/$c$ and $\pi/K$-separation from 0.8 to 2.8 GeV/$c$). Wavelength shifters (WLS) based on PMMA (poly-methyl-meta-acrylate) doped with BBQ (benzo(de)benzo(4,5)imidazo(2,1-a)isoquinolin-7-one) placed in the middle of the counters to collect Cherenkov light from the aerogel and transport its reemitted part in the condition of total internal reflection to the photon detector. As a photon detector the SiPM is considered. The main proposed and expected system parameters are the following:

- 3 layer system design: 1 layer with $n_1 = 1.03$ (2000 litres) and 2 layers with $n_2 = 1.015$ (4000 litres);
- counter dimensions are $18 \times 30 \times 8$ cm$^3$;
- WLS dimensions are $0.3 \times 28 \times 6$ cm$^3$;
- SiPM area per counter is 180 mm$^2$ (20 pixels with $3 \times 3$ mm$^2$);
- material budget for normal incidence is 14%$X_0$;
- number of counters in the system is 1 400, number of SiPMs in the system is 28 000;

- cooling system to operate with SiPMs at −40°C is required;
- 24 detected Cherenkov photons from relativistic particle ($\beta = 1$) is expected in aerogel with $n_1 = 1.03$ (8 cm) and in aerogel with $n_2 = 1.015$ (16 cm) as well;
- the main sources of subthreshold detection efficiency:
  - $\delta$-electrons production $\sim 5\%$ ($n_1 = 1.030$, 8 cm) and $\sim 3.3\%$ ($n_2 = 1.015$, 16 cm)
  - accidental coincidence with SiPM dark counts is $\sim 0.7\%$ ($n_1 = 1.030$, DCR = 70 kHz), $\sim 1.4\%$ ($n_2 = 1.015$, $DCR = 140$ kHz) in the time window of 100 ns width.

These parameters were implemented in the parametric SCT detector simulation and the capabilities of particle separation were estimated. It was shown that such system is able to provide good $\mu/\pi$-separation from 0.5 to 0.9 GeV/$c$. More detailed description of the proposed system can be found in [28, 29].

The advantages of the system in comparison with the FARICH approach are the well known production technology, less number of photon sensors, electronics channels and consequently less cost of the system.

### 3.4 DIRC-like and ToF options

The main disadvantage of the PID systems based on aerogel is the rather high momenta threshold for $\mu/\pi$-separation (about 0.4 GeV/c for aerogel with $n = 1.05$). Therefore the "ToF+ToP" (Time-of-Flight + Time-of-Propagation) and FDIRC (Focusing DIRC) options are also considered for the SCT detector project.

Today the FDIRC option is being developed for several experiments such as PANDA [30, 31], GlueX [32], EIC [33]. It was shown during the numerous R&D that the FDIRC approach is able to provide the excellent $\pi/K/p$-separation in the SCT factory operation momenta range (from 0.6 to 2.5 GeV/c) while for reliable $\mu/\pi$-separation up to 1 GeV/$c$ further improvement of this technique is required. Detailed considerations of this issue are presented in [34].

Also recent progress in the time-of-flight technique allows us to consider the ToF system for $\mu/\pi$-separation. For instance, the time resolution of about 30 ps is considered for future upgrade of the CMS detector [35], $\sigma_t \leqslant 15$ ps is the aim of the TORCH project (the time-of-flight detector for upgrade of the LHCb experiment [36]). The best time resolution about 5 ps was achieved with a detector composed of a small quartz Cherenkov radiator coupled with microchannel plate photomultiplier tube (MCP-PMT) [37]. Therefore the "ToF+ToP" technique with 30 ps intrinsic resolution were considered as additional PID subsystem which able to provide $\mu/\pi$-separation in the low momentum range. Some details and conceptual design of the "ToF+ToP" system for the SCT detector based on quartz bars ($5\times5\times250$ mm$^3$) and 1648 multi-anode MCP-PMTs with rectangular shape $40\times20$ mm are given in [28, 29]. It was shown with help of parametric simulation that such system is able to provide $\mu/\pi$-separation at the level of better than $3\sigma$ up to momentum 0.7 GeV/$c$ (see section 4).



2020 JINST 15 C04032

## 4 Comparison of PID system options

To compare the capabilities of different PID options in different momenta ranges the parametric simulation program developed for SCT detector project was used. The momentum resolution was taken from the conceptual design report [1] as following:

$$\frac{\sigma_{p_T}}{p_T} = (0.13 \pm 0.01)\% \cdot p_T + (0.45 \pm 0.03)\%, \tag{4.1}$$

where $p_T$ is the transverse momentum of the particle. For the "ToF+ToP" option $\sigma_t = 36$ ps was taken into account. This value accounts for the two effects: the counters time resolution (30 ps) and timing uncertainty of the bunch crossing (20 ps). For the ASHIPH option the parameters presented in section 3.3 were taken. FARICH separation capability was evaluated from stand-alone simulations in the GEANT4 package for the system based on 4-layer aerogel with $n_{\max} = 1.05$ and $3 \times 3\,\text{mm}^2$ photosensitive pixels. For the FDIRC option the comparison with data from [34] was performed. In figure 6 the $\mu/\pi$-separation capabilities in terms of $\sigma$ are presented for the several PID options discussed here: FARICH (•), ToF (■), ASHIPH with $n_1 = 1.030$ (▲), ASHIPH with $n_2 = 1.015$ (▼), FDIRC (○) and "ToF+ToP" (■). In the figure vertical error-bars is statistical deviation of the calculated values, horizontal error-bars correspond to the width of momentum bin for events selection. In some cases the width of the momentum bin is lees than marker size. The FARICH demonstrates the best separation power in the momenta region from 0.45 to 1.5 GeV/$c$, while ASHIPH system can provide the $\mu/\pi$-separation at the level more than $3\sigma$ only from 0.45 to

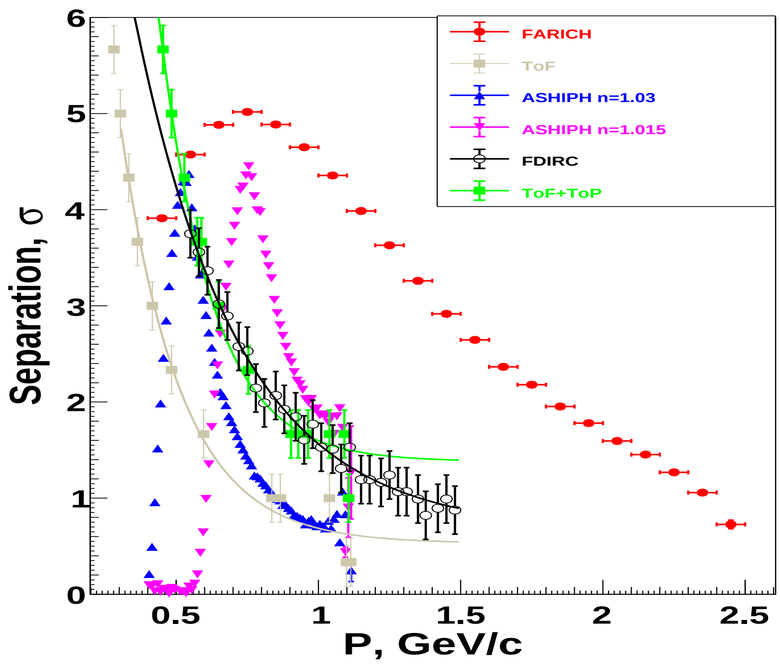


**Figure 6.** Dependence of $\mu/\pi$-separation in terms of $\sigma$ on particle momenta for different PID options: FARICH (•), ToF (■), ASHIPH with $n_1 = 1.030$ (▲), ASHIPH with $n_2 = 1.015$ (▼), FDIRC (○) and "ToF+ToP" (■).

0.9 GeV/$c$. The left cut-off (0.45 GeV/$c$) corresponds to threshold for muons in ASHIPH subsystem with $n = 1.03$ and thickness 8 cm, right edge (0.9 GeV/$c$) is determined by threshold for pions and difference of muons and pions amplitudes in ASHIPH subsystem based on aerogel with $n = 1.015$ and thickness 16 cm. Also it is shown that ToF could be complementary to FARICH or ASHIPH systems to provide $\mu/\pi$-separation below 0.4 GeV/$c$, while current achieved parameters of FDIRC and "ToF+ToP" technique is not enough to separate $\mu$ and $\pi$ at the level of $3\sigma$ above 0.7 GeV/$c$.

## 5 Summary

To provide reliable $\pi/K$-separation in the whole operational momenta range for the SCT project is more simple in comparison with $\mu/\pi$-separation for momenta range up to 1.2 GeV/$c$. Several very promising PID options which are able to provide good $\mu/\pi$-separation in the rather wide momenta range were considered in this work. Today there is no single system which is able to provide $\mu/\pi$-separation in the full desirable momenta range, while combination of the several PID approaches could do it. To achieve the good $\mu/\pi$-separation in a tracking system up to 0.22 GeV/$c$ the cluster counting mode should be implemented in DC. The FDIRC or DIRC-like-ToF systems are able to provide $\mu/\pi$-separation up to 0.7 GeV/$c$. Some optimization of the FDIRC option aimed to extend momenta range up to 1.2 GeV/$c$ is under consideration today. The use of two PID systems combined will lead to an energy resolution degradation in the calorimeter and should be carefully estimated during dtetctor development.

## Acknowledgments

The works on simulation of the SCT detector presented in section 3.1 and section 4 were supported by the Russian Science Foundation (Project no. 19-72-20114).

## References

[1] V.V. Anashin et al., *Super Charm Tau Factory, Conceptual Design Report, Part One (physics program, detector)*, BINP SB RAS, Novosibirsk, Russia (2018) [https://ctd.inp.nsk.su/wiki/images/4/47/CDR2_ScTau_en_vol1.pdf].

[2] Q. Qin et al., *Beam Dynamic Issues in the BEPCII Luminosity Comissioning*, in *Proceedings of IPAC'10*, Kyoto, Japan, 23–28 May 2010, pp. 1560–1562

[3] A.V. Bobrov and A.E. Bondar, *Search for $\tau \to \mu + \gamma$ decay at Super c-$\tau$ factory*, *Nucl. Phys. Proc. Suppl.* **225-227** (2012) 195 [arXiv:1206.1909].

[4] A.V. Bobrov and A.E. Bondar, *Feasibility study for a search for $\tau \to \mu + \gamma$ decay at Super c-$\tau$ factory*, *Nucl. Phys. Proc. Suppl.* **253-255** (2014) 199.

[5] D. Epifanov, *Measurement of Michel parameters in tau decays at the Super Charm-Tau factory with polarized electron beam*, presented at *Joint Workshop on future Charm-Tau Factory*, RAS, Moscow, Russia, 24–28 September 2019, https://c-tau.ru/indico/event/3/contributions/216/attachments/136/224/epifanov_michel_ctau19.pdf.

[6] A. Bondar, A. Grabovsky, A. Reznichenko, A. Rudenko and V. Vorobyev, *Measurement of the weak mixing angle at a Super Charm-Tau factory with data-driven monitoring of the average electron beam polarization*, *JHEP* **03** (2020) 076 [arXiv:1912.09760].

[7] A. Bobrov, *Measurement of the cross-section $e^+e^- \to n\bar{n}$ near threshold at SCTF*, presented at *Joint Workshop on future Charm-Tau Factory*, RAS, Moscow, Russia, 24–28 September 2019, https://c-tau.ru/indico/event/3/contributions/221/attachments/138/226/bobrovjf.pdf.

[8] Particle Data Group collaboration, *Review of particle physics*, http://pdg.lbl.gov/2019/hadronic-xsections/rpp2018-hadronicrpp_page1001.dat [data].

[9] P. Piminov, *Project for a Super Charm–Tau Factory at BINP*, *Phys. Part. Nucl. Lett.* **15** (2018) 732.

[10] I. Koop et al., *Longitudinal Polarization in Novosibirsk c-tau factory*, presented at *Joint Workshop on future Charm-Tau Factory*, RAS, Moscow, Russia, 24–28 September 2019, https://c-tau.ru/indico/event/3/contributions/206/attachments/183/296/Longitudinal_Polarization_in_Novosibirsk_c-tau_factory.pdf.

[11] T.V. Maltsev, L.I. Shekhtman, A.V. Sokolov and V.K. Vadakeppattu, *Simulation of different options of the Inner Tracker for Novosibirsk Super Charm-Tau Factory Detector*, *EPJ Web Conf.* **212** (2019) 01011.

[12] L. Shekhtman, F. Ignatov and V. Tayursky, *Simulation of physics background in Super c-tau factory detector*, *EPJ Web Conf.* **212** (2019) 01009.

[13] K. Todyshev, *Drift chamber R&D progress in Novosibirsk*, presented at *Joint Workshop on future Charm-Tau Factory*, RAS, Moscow, Russia, 24–28 September 2019, https://c-tau.ru/indico/event/3/contributions/183/attachments/163/259/dcctd2019.pdf.

[14] F. Grancagnolo, *State-of-the-art of Drift chambers*, presented at *CREMLIN WP7 "Super c-tau factory workshop"*, BINP, Novosibirsk, Russia, 26–27 May 2018, https://indico.inp.nsk.su/event/13/session/12/contribution/14/material/slides/0.pdf.

[15] E. Prokhorova, *Study of the fast calorimeter prototype for the Super Charm-Tau Factory*, *EPJ Web Conf.* **212** (2019) 01007.

[16] T. Uglov, *Proposal of the Muon System for the Super Tau-Charm Factory*, *EPJ Web Conf.* **212** (2019) 01010.

[17] MEG II collaboration, *The design of the MEG II experiment*, *Eur. Phys. J.* **C 78** (2018) 380 [arXiv:1801.04688].

[18] BaBar collaboration, *The BaBar detector*, *Nucl. Instrum. Meth.* **A 479** (2002) 1 [hep-ex/0105044].

[19] A. Yu. Barnyakov, M. Yu. Barnyakov, V.S. Bobrovnikov, A.R. Buzykaev, A.F. Danilyuk, V.L. Kirillov et al., *Focusing aerogel RICH (FARICH)*, *Nucl. Instrum. Meth.* **A 553** (2005) 70.

[20] S. Nishida et al., *Aerogel RICH for the Belle II forward PID*, *Nucl. Instrum. Meth.* **A 766** (2014) 28.

[21] A. Yu. Barnyakov et al., *Beam test of FARICH prototype with Digital Photon Counter*, *Nucl. Instrum. Meth.* **A 732** (2013) 352.

[22] A. Yu. Barnyakov et al., *Aerogel for FARICH detector*, *Nucl. Instrum. Meth.* **A 766** (2014) 235.

[23] A.Yu. Barnyakov, et al., *PID system based on focusing aerogel RICH for the super c-τ factory*, *Nucl. Instrum. Meth.* **A 952** (2020) 162247.

[24] A. Onuchin, A. Shamov, Yu. Skovpen, A. Vorobov, A. Danilyuk, T. Gorodetskaya et al., *The Aerogel Cherenkov counters with wavelength shifters and phototubes*, *Nucl. Instrum. Meth.* **A 315** (1992) 517.

[25] A.Y. Barnyakov et al., *Operation and performance of the ASHIPH counters at the KEDR detector*, *Nucl. Instrum. Meth.* **A 824** (2016) 79.

[26] A. Yu. Barnyakov et al., *Particle identification system based on dense aerogel*, Nucl. Instrum. Meth. **A 732** (2013) 330.

[27] A. Yu. Barnyakov et al., *Testing aerogel Cherenkov counters with $N = 1.05$ using electrons and muons*, Instrum. Exp. Tech. **58** (2015) 30.

[28] A.Yu. Barnyakov et al., *The Super C-$\tau$ Factory particle identification system options*, EPJ Web Conf. **212** (2019) 01012.

[29] A.Yu. Barnyakov, et al., *Particle identification system for the super charm–tau factory at novosibirsk*, Nucl. Instrum. Meth. **A 958** (2020) 162352.

[30] C. Schwarz et al., *The Barrel DIRC detector of PANDA*, Nucl. Instrum. Meth. **A 936** (2019) 586 [arXiv:1901.08432].

[31] K. Föhl et al., *The Endcap Disc DIRC detector of PANDA*, Nucl. Instrum. Meth. **A 936** (2019) 588.

[32] M. Patsyuk et al., *Status of the GlueX DIRC*, Nucl. Instrum. Meth. **A 952** (2020) 161756.

[33] G. Kalicy et al., *High-performance DIRC detector for the future Electron Ion Collider experiment*, 2018 *JINST* **13** C04018.

[34] M. Schmidt, M. Düren, A. Hayrapetyan, A. Yu. Barnyakov and S.A. Kononov, *DIRC options for the Super Charm Tau Factory*, 2020 *JINST* **15** C02032.

[35] M. Lucchini, *Development of the CMS MIP timing detector*, Nucl. Instrum. Meth. **A 958** (2020) 162090.

[36] N. Harnew et al., *TORCH: a large area time-of-flight detector for particle identification*, Nucl. Instrum. Meth. **A 936** (2019) 595 [arXiv:1810.06658].

[37] K. Inami, N. Kishimoto, Y. Enari, M. Nagamine and T. Ohshima, *A 5-ps TOF-counter with an MCP-PMT*, Nucl. Instrum. Meth. **A 560** (2006) 303.


2020 JINST 15 C04032